Network of families of symmetric spatial periodic orbits in the Hill problem via symplectic invariants

Cengiz Aydin[1], Alexander Batkhin[2]
cengiz.aydin@hotmail.de, batkhin@technion.ac.il

[1] *Institut für Mathematik, Universität Heidelberg, Germany*
[2] *Techion – Israel Institute of Technology, Haifa, Israel*

AMCM-2024, August 19–24, 2024

Talk outlook

1. Circular Hill Problem, its symmetries and basic families
2. On symplectic invariants
3. Interconnections between the basic families
4. Conclusion

Abstract

A technique of Conley–Zehnder indices is applied for investigation of interconnections of the basic families of periodic orbits with maximal numbers of symmetries of the well-known Hill problem. These basic families are g, f – families of planar direct and retrograde periodic orbits, and $\mathcal{B}_0$ – family of rectilinear vertical consecutive collision orbits. The relations among families of periodic orbits are provided by families of spatial symmetric periodic orbits which makes k-covering at the bifurcation points. All the families form a common network and can be represented as well-organized bifurcation graphs of the interconnectedness.

Hierarchy of celestial-mechanical problems

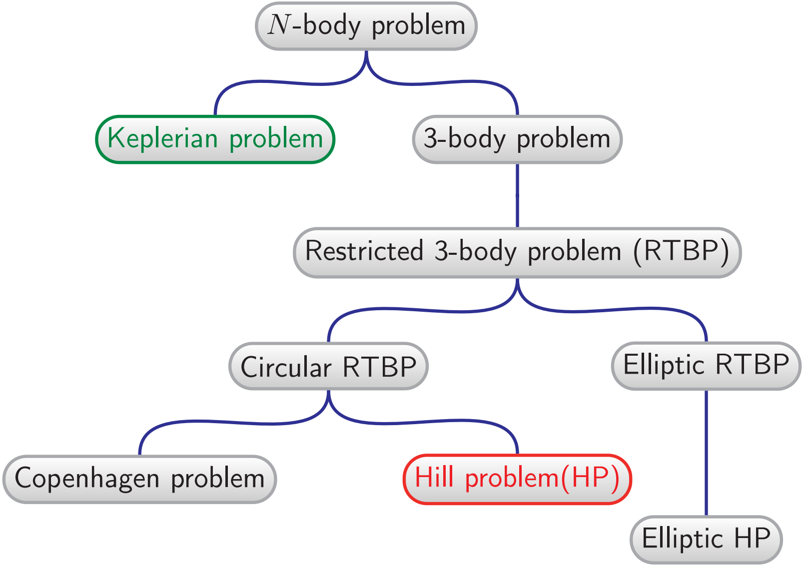

Circular Hill Proble

The ***Hill three-body problem*** (Hill3BP), a limiting case of the ***circular restricted three-body problem*** (CR3BP), is a well-known model which provides an approximation of the dynamics of the infinitesimal body in the vicinity of the smaller primary.

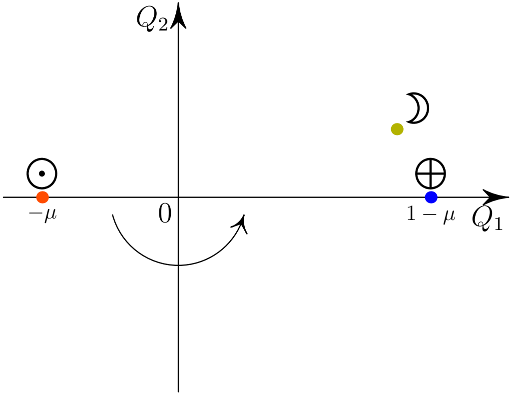

Circular Hill Proble

The ***Hill three-body problem*** (Hill3BP), a limiting case of the ***circular restricted three-body problem*** (CR3BP), is a well-known model which provides an approximation of the dynamics of the infinitesimal body in the vicinity of the smaller primary.

The remaining primary is pushed infinitely far away in a way that it acts as a velocity independent gravitational perturbation of the rotating Kepler problem formed by the smaller primary and the infinitesimal body.

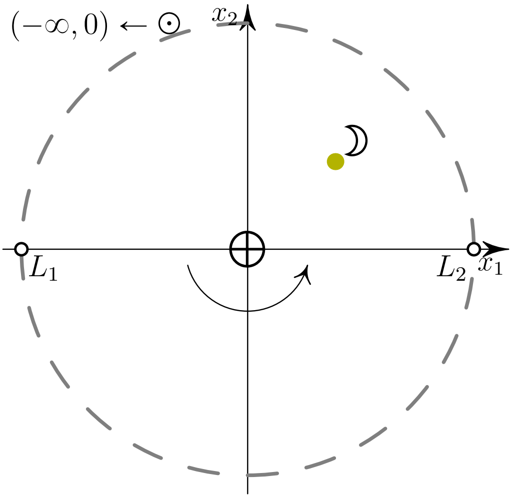

Applications of the Hill3BP

In its original application, George Hill reformulated the lunar theory and discovered a periodic solution with period equal to the synodic month of the Moon.

Main applications of Hill's approach such as

- capturing in the dynamics of natural or artificial satellites,
- distant moons of asteroids,
- low-energy escaping trajectories,
- frozen orbits around planetary satellites.

Hill3BP problem's periodic solution can be continued to CR3BP or even into three-body problem solutions and thus can be used in astrodynamical projects.

Hamiltonian of the Hill3BP

The Hamiltonian form of the CR3BP is

$$H(x, y, z, p_x, p_y, p_z) = \frac{1}{2}\left(p_x^2 + p_y^2 + p_z^2\right) - \frac{1-\mu}{r_1} - \frac{\mu}{r_2} + p_x y - p_y x,$$

which has an equivalent ***Jacobi integral*** defined by $\Gamma = -2H$.

Hamiltonian of the Hill3BP

The Hamiltonian form of the CR3BP is

$$H(x,y,z,p_x,p_y,p_z) = \frac{1}{2}\left(p_x^2+p_y^2+p_z^2\right) - \frac{1-\mu}{r_1} - \frac{\mu}{r_2} + p_x y - p_y x,$$

which has an equivalent ***Jacobi integral*** defined by $\Gamma = -2H$.

For $\mu \ll 1$, the smaller primary is shifted to the origin, making blowing-up of coordinates by a factor $\mu^{1/3}$ and after tending $\mu \to 0$ getting Hill3BP problem Hamiltonian

$$H(x,y,z,p_x,p_y,p_z) = \frac{1}{2}\left(p_x^2+p_y^2+p_z^2\right) - \frac{1}{r} + p_x y - p_y x - x^2 + \frac{1}{2}\left(y^2+z^2\right).$$

Hamiltonian of the Hill3BP

The Hamiltonian form of the CR3BP is

$$H(x,y,z,p_x,p_y,p_z) = \frac{1}{2}\left(p_x^2 + p_y^2 + p_z^2\right) - \frac{1-\mu}{r_1} - \frac{\mu}{r_2} + p_x y - p_y x,$$

which has an equivalent ***Jacobi integral*** defined by $\Gamma = -2H$.

For $\mu \ll 1$, the smaller primary is shifted to the origin, making blowing-up of coordinates by a factor $\mu^{1/3}$ and after tending $\mu \to 0$ getting Hill3BP problem Hamiltonian

$$H(x,y,z,p_x,p_y,p_z) = \frac{1}{2}\left(p_x^2 + p_y^2 + p_z^2\right) - \frac{1}{r} + p_x y - p_y x - x^2 + \frac{1}{2}\left(y^2 + z^2\right).$$

It consists of the rotating Kepler problem Hamiltonian with a gravitational perturbation produced by the massive primary. This difference between the rotating Kepler problem and Hill3BP system gives a dramatic dynamical change, turning the Hill3BP a non-integrable.

Symmetries

Equations of motion derived from (1) are invariant under discrete group $\mathbb{Z}_2 \times \mathbb{Z}_2 \times \mathbb{Z}_2$ of symplectic (anti-symplectic) symmetries ρ of the extended phase space:

$$\rho_{\alpha\beta\gamma} : (t, x, y, z, p_x, p_y, p_z) \to (\alpha t, \beta x, \alpha\beta y, \gamma z, \alpha\beta p_x, \beta p_y, \alpha\gamma p_z), \qquad (1)$$

where $\alpha, \beta, \gamma \in \{+1, -1\}$. So all solutions to the Hill3BP can be divided into groups with different number of symmetries (1).

The symmetry of a periodic solution plays an essential role in understanding dynamics of the problem.

Basic families of periodic solutions

Conjecture

Families of orbits with maximal number of symmetries form a kind of backbone for a network of periodic solution

Basic families of periodic solutions

Conjecture

Families of orbits with maximal number of symmetries form a kind of backbone for a network of periodic solution

Three basic families, whose orbits are simple and have the largest number of symmetries:

Basic families of periodic solutions

Conjecture

Families of orbits with maximal number of symmetries form a kind of backbone for a network of periodic solution

Three basic families, whose orbits are simple and have the largest number of symmetries:

- g and f are families of planar ***direct*** and retrograde satellite [Hénon, 1969],

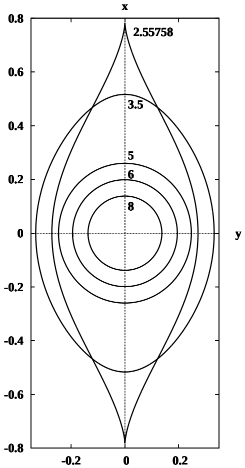

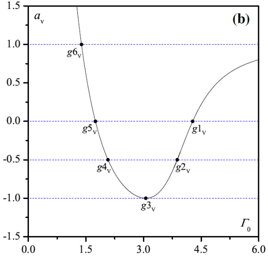

Basic families of periodic solutions

Conjecture

Families of orbits with maximal number of symmetries form a kind of backbone for a network of periodic solution

Three basic families, whose orbits are simple and have the largest number of symmetries:

- g and f are families of planar direct and ***retrograde*** satellite [Hénon, 1969],

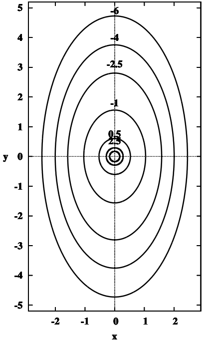

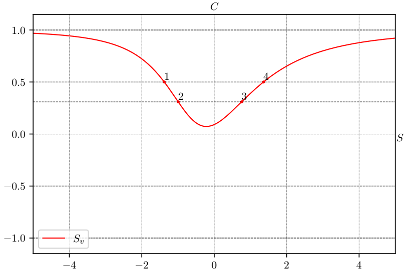

Basic families of periodic solutions

Conjecture

Families of orbits with maximal number of symmetries form a kind of backbone for a network of periodic solution

Three basic families, whose orbits are simple and have the largest number of symmetries:

- g and f are families of planar direct and retrograde satellite [Hénon, 1969],
- $\mathcal{B}_0$ is a family of ***vertical collision orbits*** [Lidov, 1982]

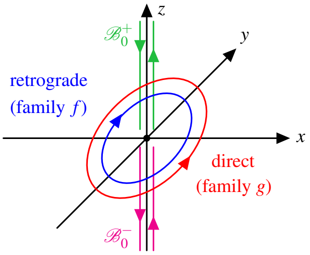

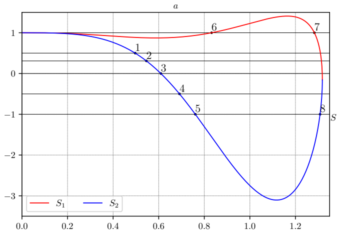

Basic families of periodic solutions

Conjecture

Families of orbits with maximal number of symmetries form a kind of backbone for a network of periodic solution

Other important families are

- ***Lyapunov families*** a ***(***c***)*** emanating from L_1 (L_2)

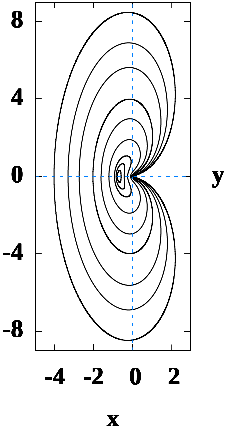

Basic families of periodic solutions

Conjecture

Families of orbits with maximal number of symmetries form a kind of backbone for a network of periodic solution

Other important families are

- Lyapunov families a (c) emanating from L_1 (L_2)
- family g' appeared after symmetry breaking bifurcation of g

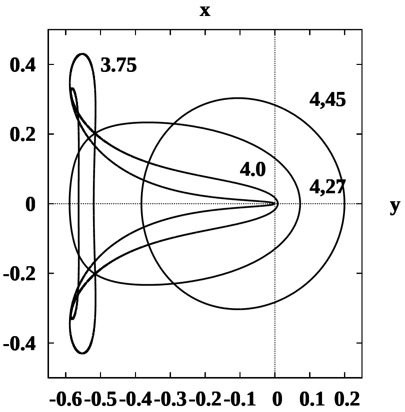

Basic families of periodic solutions

Conjecture

Families of orbits with maximal number of symmetries form a kind of backbone for a network of periodic solution

Other important families are

- Lyapunov families a (c) emanating from L_1 (L_2)
- family g' appeared after symmetry breaking bifurcation of g
- family f_3 gives twice 3-covering of the family f

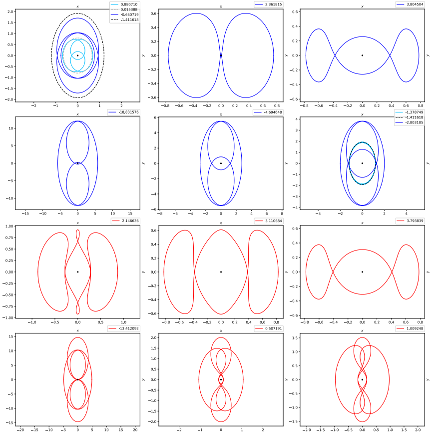

Basic families of periodic solutions

Conjecture

Families of orbits with maximal number of symmetries form a kind of backbone for a network of periodic solution

Other important families are

- Lyapunov families a (c) emanating from L_1 (L_2)
- family g' appeared after symmetry breaking bifurcation of g
- family f_3 gives twice 3-covering of the family f
- ***Lyapunov eight-form*** spatial family

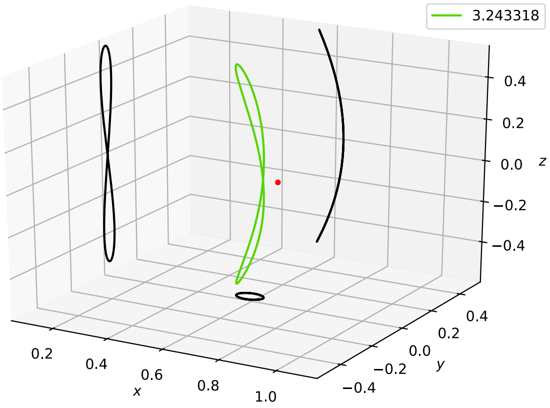

Goal of the work

It was shown in [A. B. Batkhin, Batkhina, 2009] that all these families are connected to each other by families of spatial periodic orbits and form a kind of common network.

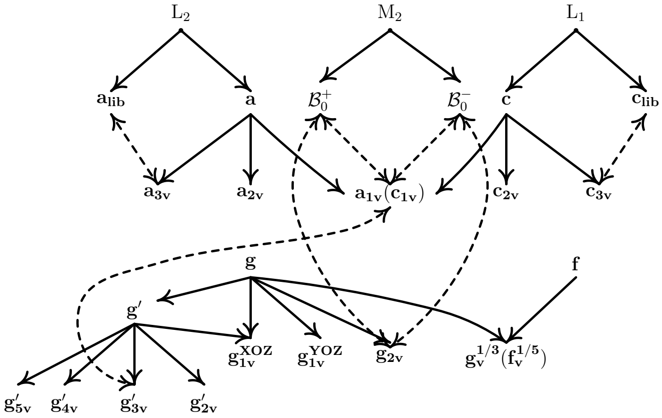

Goal of the work

It was shown in [A. B. Batkhin, Batkhina, 2009] that all these families are connected to each other by families of spatial periodic orbits and form a kind of common network.

Current work significantly extends these results by systematically applying the technique of ***symplectic invariants***.

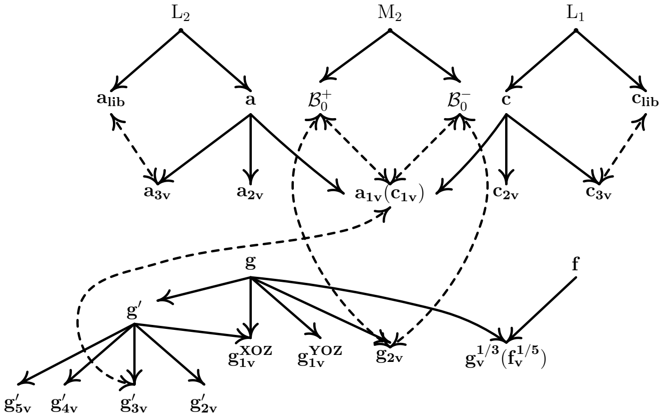

On symplectic invariants

- Conley–Zehnder index μ_{CZ} of periodic orbits
- Krein signature
- Local Floer homology and its Euler characteristic (bifurcation-invariant)

Conley–Zehnder index μ_{CZ} of periodic orbits

- The Conley–Zehnder index [Conley, Zehnder, 1984], [Salamon, Zehnder, 1992] assigns a mean winding number to non-degenerate periodic orbits, defined in terms of a path of symplectic matrices $\Psi(t)$ generated by the linearized flow along the whole periodic orbit (transverse to the direction of the Hamiltonian vector field).
- This symplectic path $\Psi(t)$ starts at the identity and ends at the reduced monodromy.
- The set of symplectic matrices with eigenvalue 1 is called "Maslov cycle", which corresponds to the space of reduced monodromies that are degenerate. μ_{CZ} measures the twisting of the symplectic path $\Psi(t)$ by counting the number of crossing the Maslov cycle that lies between the starting point of a periodic orbit and its end point.

μ_{CZ} of planar periodic orbits in the planar system

- Let ξ^n be the n-times iteration of a planar orbit ξ. Assume that ξ^n is non-degenerate for all $n \geqslant 1$. The reduced monodromy of ξ^n is an element of $Sp(2) = SL(2, \mathbb{R})$.
- **Elliptic case**. The Floquet multipliers are of the form $e^{\pm in\theta}$ and the reduced monodromy is conjugate to a rotation in $\mathbb{R}^2$ of the form $\begin{pmatrix} \cos n\theta & -\sin n\theta \\ \sin n\theta & \cos n\theta \end{pmatrix}$. In particular,

$$\mu_{CZ}(\xi^n) = 1 + 2 \cdot \lfloor n \cdot \theta/(2\pi) \rfloor =: 1 + 2 \cdot \mathrm{rot}(\xi^n).$$

- **Hyperbolic case**. The Floquet multipliers are positive or negative real and of the form λ and $1/\lambda$. Then the corresponding eigenvectors are rotated by $m\pi$ for an integer m, and

$$\mu_{CZ}(\xi^n) = nm, \quad m \in \begin{cases} 2\mathbb{Z} & \text{for the pos. hyperbolic case} \\ 2\mathbb{Z}+1 & \text{for the neg. hyperbolic case.} \end{cases}$$

Index jump at bifurcation point

The index is constant along an orbit cylinder, parametrized by the energy. If a periodic orbit becomes degenerate, bifurcation occurs and the index jumps according to direction of crossing the eigenvalue 1.

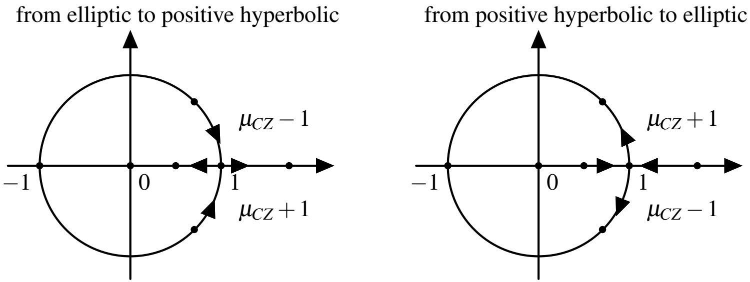

Natural question to ponder:

"How to determine the direction of crossing the eigenvalue 1?"

Krein signature

- The classical Krein signature [Arnold, Avez, 1968] associates a $\pm$ sign to each pair of elliptic Floquet multipliers of the form $e^{\pm i\theta}$. We use the Krein signature for symmetric periodic orbits that was constructed in [Frauenfelder, Moreno, 2023], which assigns a $\pm$ sign to each elliptic and hyperbolic Floquet multiplier, and coincides with the classical one in the elliptic case.
- This signature is invariant under the choice of the symplectic basis to write down the (reduced) monodromy matrix.
- Especially, it determines the direction of the rotation, meaning that if the rotation is determined by $+\theta$ or $-\theta$. Therefore, the Krein signature specifies the direction of crossing the eigenvalue 1 and thereby the index jump.

Determination of Conley–Zehnder indices

- Instead of using directly the formal definition, we determine the index by studying analytically the origin of the natural families of periodic orbits, continue those families for higher energies and study their interaction at bifurcation points as described before.
- Planar periodic orbits in the spatial system has planar and spatial Floquet multipliers, and planar and spatial Conley–Zehnder indices.
- For very low energies, the regularized Kepler problem is the source of the families g, f and $\mathcal{B}_0^{\pm}$. It was shown in [Aydin, 2023a] that for very low energies, their indices are given by

$$\mu_{CZ} = \begin{cases} 6 = \mu_{CZ}^p + \mu_{CZ}^s = 3+3 & \text{for } g \\ 4 & \text{for } \mathcal{B}_0^{\pm} \\ 2 = \mu_{CZ}^p + \mu_{CZ}^s = 1+1 & \text{for } f. \end{cases}$$

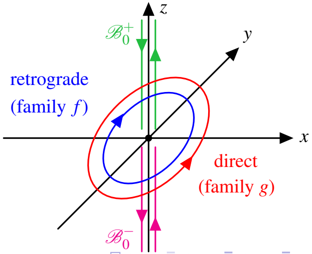

Jump of planar index generates planar-to-planar bifurcation, and jump of spatial index generates planar-to-spatial bifurcation.

Conley–Zehnder indices of planar and vertical Lyapunov orbits

- It is well-known that the analysis of the linear behavior of the flow around collinear Lagrange points is of the type saddle $\times$ center $\times$ center.
- The planar and vertical frequencies ω_p and ω_v, related to both centers, satisfy

$$\omega_v < \omega_p < 2\omega_v.$$

- Therefore, in the vicinity of the collinear Lagrange points it holds that

$$\mu_{CZ} = \begin{cases} 3 = \mu^p_{CZ} + \mu^s_{CZ} = 2 + 1 & \text{for the family of planar Lyapunov orbits} \\ 5 & \text{for the family of vertical Lyapunov orbits.} \end{cases}$$

Local Floer homology and its Euler characteristic (bifurcation-invariant)

- Euler characteristic of closed surfaces equals $V - E + F$ in a triangulation (topological invariant).

dimension	0	1	2
	V	E	F

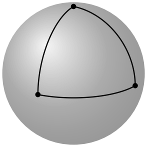

For the sphere:
$V - E + F = 2$

- More generally, for any topological space, the Euler characteristic is defined as the alternating sum of the rank of the (singular) homology groups.
- **Local Floer homology.** The Conley–Zehnder index leads to a grading on local Floer homology. Fascinatingly, the local Floer homology and its Euler characteristic stay invariant under bifurcation points [Ginzburg, 2010]. Thus, ***the index provides important information how different families are related to each other at bifurcation points***.
- "Bad orbits" (notation from SFT) do not count to the local Floer homology. They appear as even covers of periodic orbits with exactly one pair of neg. hyperb. Floquet multipliers.

Astronomical significance of Conley–Zehnder indices

The period of Hill's lunar orbit corresponds to the synodic month, which is around 29.5305 days. Planar and spatial elliptic Floquet multipliers are

$$e^{\pm i\theta_p}, \quad \theta_p = 0.450390, \quad e^{\pm i\theta_s}, \quad \theta_s = 0.534613.$$

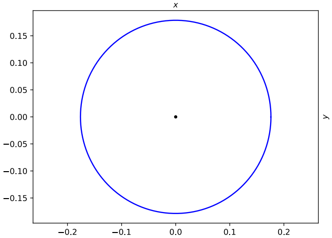

It was shown in [Aydin, 2023a] that the anomalistic and draconitic months can be expressed in terms of the CZ indices and rotation angles. The indices associated to Hill's lunar orbit are

$$\mu_{CZ}^p = \mu_{CZ}^s = 3, \quad \text{rot}^p = \text{rot}^s = 1.$$

Krein signatures of elliptic Floquet multipliers indicate that each rotation is determined by $+\theta_p$ and $+\theta_s$. The computation of the time for a planar and spatial rotation during one synodic month yields 27.5529 days (anomalistic month) and 27.2126 days (draconitic month). Knowledge of these lunar months date back to the Babylonians until around 500 BCE.

Summary of investigations

We provide bifurcation graphs illustrated a common network in association to the natural families of periodic orbits and their bifurcations, based on the technique of symplectic invariants.

To be emphasized is that our investigations show the following structures of bifurcation results of families of spatial orbits in each row.

g'	g	$\mathcal{B}_0^{\pm}$	f	f_3	halo
1					2
	1	2			
2	2	3			
3	3	4	5	1	
4	4	5	6	2	
	5	6	7		

Bifurcation graph associated to g and g'

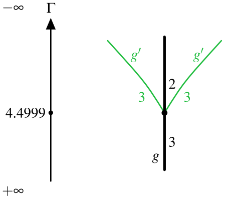

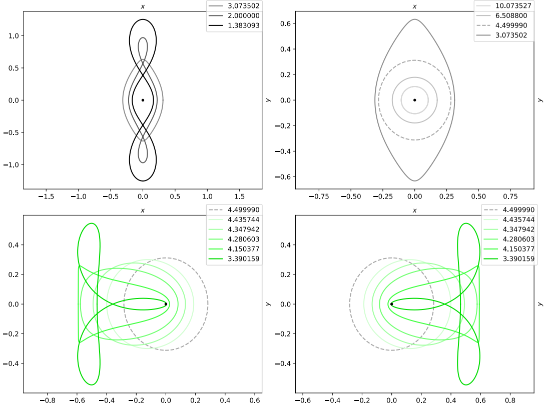

Euler characteristics (with respect to planar indices) before and after bifurcation are

$$(-1)^3 = -1, \quad (-1)^2 + 2 \cdot (-1)^3 = -1.$$

Connection between g and double cover of $\mathcal{B}_0^{\pm}$

At $\Gamma = 1.383093$ the spatial index of g-orbits jumps from 3 to 4 (planar index is 2). The continuation of the new branch of spatial orbits terminates, after an index jump at $\Gamma = -0.072698$, at the double cover of $\mathcal{B}_0^{\pm}$ at $\Gamma = -0.182001$.

Notice that $\overline{5}$ indicates bad orbits, which are ignored in the local Floer homology and not counted.

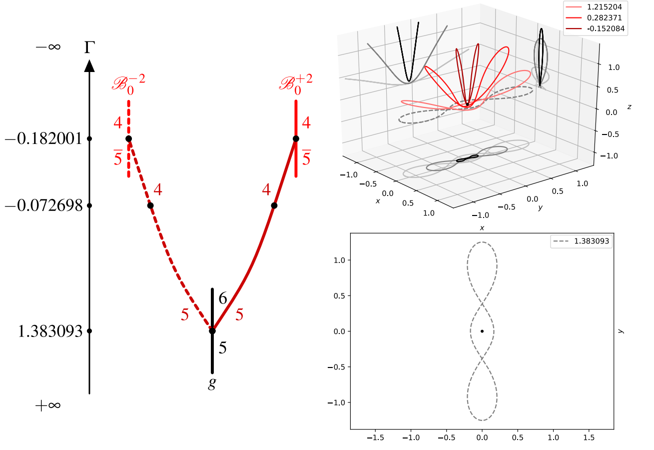

Connection between g' and double cover of halo orbits

Next result shows the connection between g' and double cover of halo orbits. Verification of bifurcation points:

- At $\Gamma = 3.390159$ the Euler characteristics before and after bifurcation are $(-1)^6 = 1$ and $2 \cdot (-1)^6 + (-1)^7 = 1$.
- At $\Gamma = 1.095146$ the Euler characteristics are $(-1)^6 = 1$ before and after bifurcation. Notice that the index $\overline{7}$ indicates bad orbits, which are ignored in the local Floer homology and not counted.

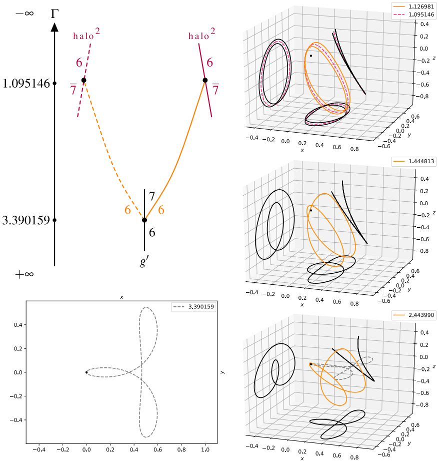

Bifurcation graph between g, g', $\mathcal{B}_0^{\pm}$, f, and $\mathbf{f}_3$

Here connections formed by spatial orbits that bifurcate from

- triple cover of g and g',
- fourth cover of $\mathcal{B}_0^{\pm}$,
- fifth cover of f and
- simple cover of $\mathbf{f}_3$.

The corresponding bifurcation graph is illustrated in Figure.

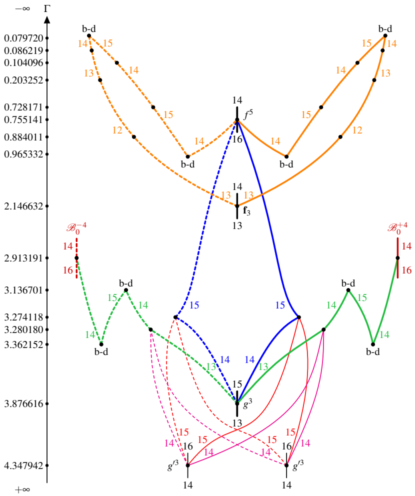

Bifurcation graph between g, g', $\mathcal{B}_0^{\pm}$, f, and f_3

At $\Gamma = 3.876616$ μ_{CZ} of its triple cover jumps from 13 to 15 (the planar index is 6 and the spatial index jumps from 7 to 9). From the triple cover there bifurcates two families of spatial orbits, one has index 14 (blue family) and one has index 13 (green family).

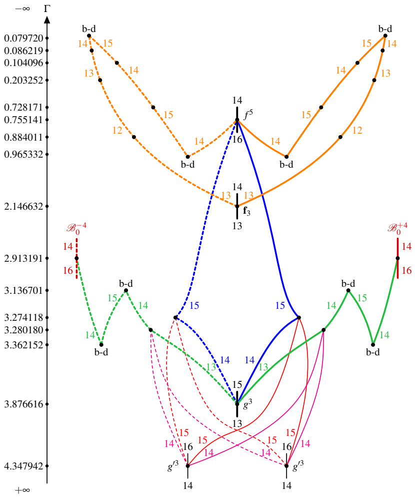

Bifurcation graph between g, g', $\mathcal{B}_0^{\pm}$, f, and f_3

At $\Gamma = 3.876616$ μ_{CZ} of its triple cover jumps from 13 to 15 (the planar index is 6 and the spatial index jumps from 7 to 9). From the triple cover there bifurcates two families of spatial orbits, one has index 14 (blue family) and one has index 13 (green family).

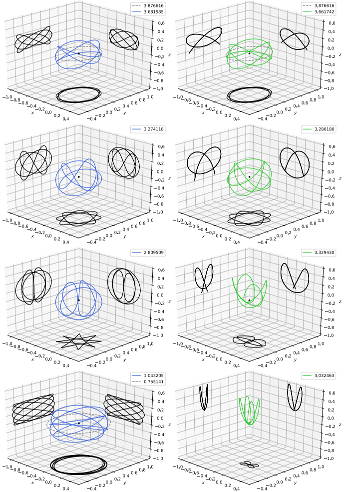

Bifurcation graph between g, g', $\mathcal{B}_0^{\pm}$, f, and f_3

The orbits of the blue family are doubly symmetric with respect to the OX-plane and OY-plane, and they terminate at $\Gamma = 0.755141$ corresponding to fifth cover spatial bifurcation of f where the index jumps from 16 to 14. The blue orbits undergo an index jump from 14 to 15 at $\Gamma = 3.274118$.

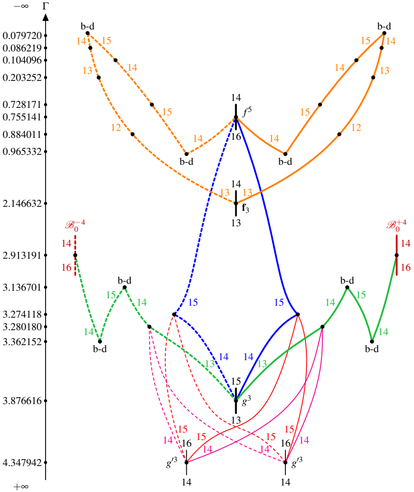

Bifurcation graph between g, g', $\mathcal{B}_0^{\pm}$, f, and f_3

The green orbits are doubly symmetric with respect to the XOZ-axis and YOZ-axis. Our studies in the regularized problem show that this collision point corresponds to a branch that bifurcate from fourth cover of $\mathcal{B}_0^{\pm}$ (where the index jumps from 16 to 14). Furthermore, the green orbits make an index jump from 13 to 14 at $\Gamma = 3.280180$, and then they undergo two times a birth-death bifurcation, first at $\Gamma = 3.136701$ and second at $\Gamma = 3.362152$.

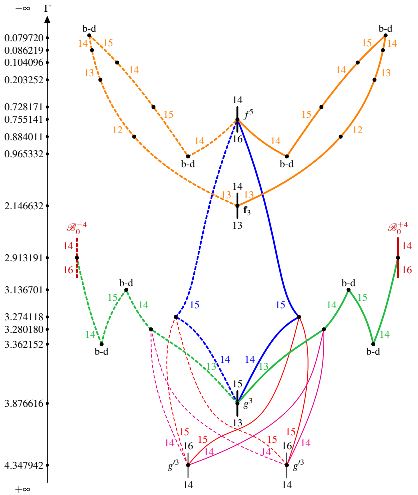

Bifurcation graph between g, g', $\mathcal{B}_0^{\pm}$, f, and f_3

At $\Gamma = 4.347942$ the triple cover of g' generates two families of spatial orbits (red and purple family). At this bifurcation point the index jumps from 14 to 16, and the red family has index 15 (orbits are simple symmetric with respect to the OX-axis) and the purple family has index 14 (orbits are simple symmetric with respect to the OY-axis). It was investigated in [Aydin, 2023b], by using the indices and symmetry properties, that red family meets blue family and purple family meets green family (note that by pure computation of red and purple family, one starts at g' and terminates at its symmetric g' orbit).

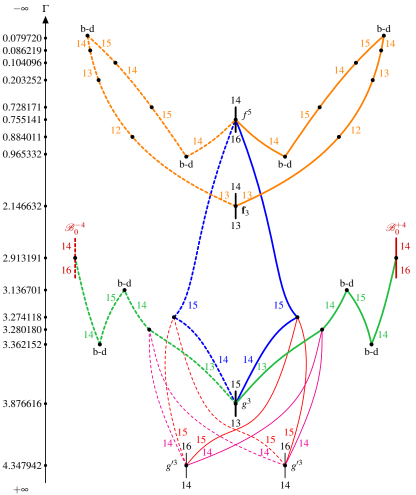

Bifurcation graph between g, g', $\mathcal{B}_0^{\pm}$, f, and f_3

At $\Gamma = 4.347942$ the triple cover of g' generates two families of spatial orbits (red and purple family). At this bifurcation point the index jumps from 14 to 16, and the red family has index 15 (orbits are simple symmetric with respect to the OX-axis) and the purple family has index 14 (orbits are simple symmetric with respect to the OY-axis). It was investigated in [Aydin, 2023b], by using the indices and symmetry properties, that red family meets blue family and purple family meets green family (note that by pure computation of red and purple family, one starts at g' and terminates at its symmetric g' orbit).
Some red and purple orbits are plotted in Figure to the right.

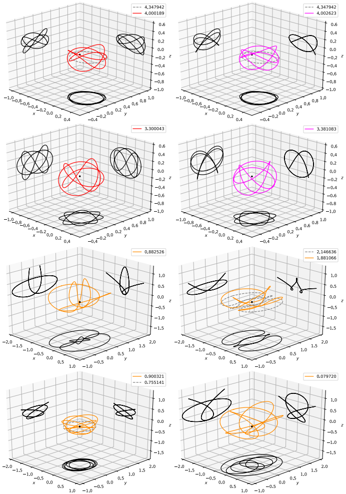

Bifurcation graph between g, g', $\mathcal{B}_0^{\pm}$, f, and $\mathbf{f}_3$

At $\Gamma = 2.146632$ a branch of spatial orbits bifurcation from $\mathbf{f}_3$ terminates at $\Gamma = 0.755141$ at fifth cover of f. This branch is the orange family in Figure 27, which undergoes two birth-death bifurcations and several index jumps in between.

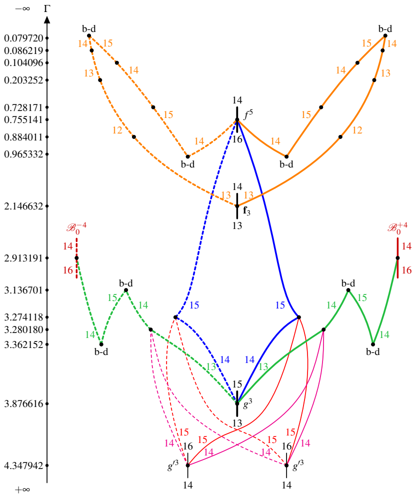

Bifurcation graph between g, g', $\mathcal{B}_0^{\pm}$, f, and $\mathbf{f}_3$

At $\Gamma = 2.146632$ a branch of spatial orbits bifurcation from $\mathbf{f}_3$ terminates at $\Gamma = 0.755141$ at fifth cover of f. This branch is the orange family in Figure 27, which undergoes two birth-death bifurcations and several index jumps in between.

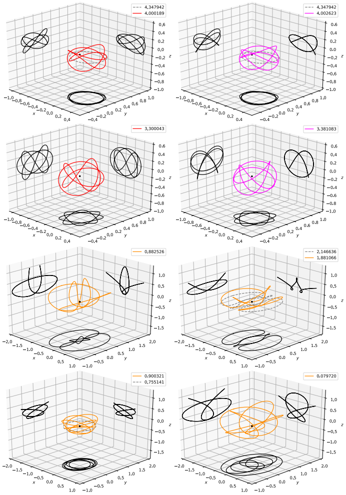

Bifurcation graph between g, g', $\mathcal{B}_0^{\pm}$, f, and $\mathbf{f}_3$

As a conclusion, the part of the network related to blue, green (without $\mathcal{B}_0^{\pm}$), red and purple family was already constructed in [Aydin, 2023b], based on computations from [Kalantonis, 2020]. We completed this network by exploring the families $\mathcal{B}_0^{\pm}$ and $\mathbf{f}_3$ and their relations at bifurcation points.

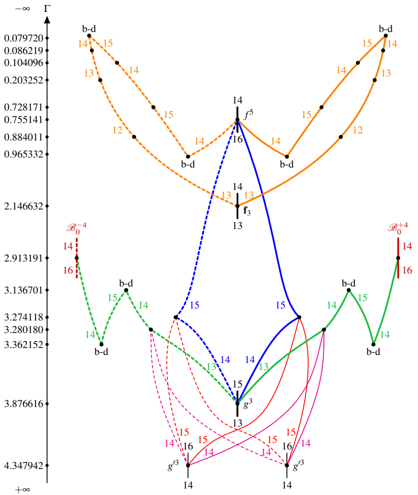

Conclusion

Based on ***symplectic invariants***, we provide bifurcation graphs illustrated a common network in association to the natural families of periodic orbits and their bifurcations. A full description of our results [Aydin, A. Batkhin, 2024] is in progress.

We have presented some of the structures of bifurcation results of families of spatial orbits. In particular, such pattern can be expected in view of their indices:
Recall that for very low energies, g has index 6, $\mathcal{B}_0^{\pm}$ has index 4 and f has index 2. These indices show that, for connections between g, $\mathcal{B}_0^{\pm}$ and f, one should examine the corresponding n-th, $n+1$-th and $n+2$-th cover, which we have investigated for $n = 3,4,5$.

g'	g	$\mathcal{B}_0^{\pm}$	f	f_3	halo
1					2
	1	2			
2	2	3			
3	3	4	5	1	
4	4	5	6	2	
	5	6	7		

References (1)

Arnold V., Avez A. Ergodic Problems of Classical Mechanics. New York, Benjamin, 1968.

Aydin C., Batkhin A. Network of families of symmetric spatial periodic orbits in the Hill problem via symplectic invariants. // In progress. 2024.

Aydin C. From Babylonian lunar observations to Floquet multipliers and Conley–Zehnder indices. // Journal of Mathematical Physics. 2023a. Aug. Vol. 64, no. 8. ISSN 1089-7658. DOI: 10.1063/5.0156959. URL: http://dx.doi.org/10.1063/5.0156959.

Aydin C. The Conley–Zehnder indices of the spatial Hill three-body problem. // Celestial Mechanics and Dynamical Astronomy. 2023b. Vol. 135, no. 3. ISSN 1572-9478. DOI: 10.1007/s10569-023-10134-7.

Batkhin A. B., Batkhina N. V. Hierarchy of periodic solutions families of spatial Hill's problem. // Solar System Research. 2009. Apr. Vol. 43, no. 2. P. 178–183. ISSN 1608-3423. DOI: 10.1134/s0038094609020105. URL: http://dx.doi.org/10.1134/S0038094609020105.

References (2)

Conley C., Zehnder E. Morse-type index theory for flows and periodic solutions for Hamiltonian Equations. // Communications on Pure and Applied Mathematics. 1984. Mar. Vol. 37, no. 2. P. 207–253. ISSN 1097-0312. DOI: 10.1002/cpa.3160370204. URL: http://dx.doi.org/10.1002/cpa.3160370204.

Frauenfelder U., Moreno A. On GIT quotients of the symplectic group, stability and bifurcations of periodic orbits (with a view towards practical applications). // Journal of Symplectic Geometry. 2023. Vol. 21, no. 4. P. 723–773. DOI: 10.4310/JSG.2023.v21.n4.a3. URL: https://dx.doi.org/10.4310/JSG.2023.v21.n4.a3.

Ginzburg V. L. The Conley conjecture. // Annals of Mathematics. 2010. Vol. 172, no. 2. P. 1127. ISSN 0003-486X. DOI: 10.4007/annals.2010.172.1127. URL: http://dx.doi.org/10.4007/annals.2010.172.1127.

Hénon M. Numerical exploration of the restricted problem V. Hill's case: periodic orbits and their stability. // Astron. & Astrophys. 1969. Vol. 1. P. 223–238.

References (3)

Kalantonis V. S. Numerical Investigation for Periodic Orbits in the Hill Three-Body Problem. // Universe. 2020. May. Vol. 6, no. 6. P. 72. ISSN 2218-1997. DOI: 10.3390/universe6060072. URL: http://dx.doi.org/10.3390/universe6060072.

Lidov M. L. A method of construction of families of spatial periodic orbits in Hill's problem. // Kosmicheskie Issledovaniia. 1982. Nov. Vol. 20. P. 787–807. (in Russian).

Salamon D., *Zehnder E.* Morse theory for periodic solutions of hamiltonian systems and the maslov index. // Communications on Pure and Applied Mathematics. 1992. Vol. 45. P. 1303–1360. DOI: 10.1002/cpa.3160451004. URL: https://doi.org/10.1002/cpa.3160451004.

Thanks for your attention!